Ultraviolet and violet upconversion luminescence in Er^{3+}-doped yttrium aluminum garnet crystals

Huailiang Xu and Zhankui Jiang
Department of Physics, Jilin University, Jiefang road 119, ChangChun 130023, People's Republic of China
(Received 18 January 2002; revised manuscript received 28 March 2002; published 3 July 2002)

The ultraviolet and violet upconverted luminescence around 320, 410, and 470 nm in Er^{3+}-doped yttrium aluminum garnet has been observed at room temperature with a tunable OPO laser excitation. The upconversion mechanisms upon $^4S_{3/2}$ excitation ($\approx$545 nm) are investigated by means of the decay profiles of upconvered luminescence and excitation spectrum. It appears that, depending on the excited wavelength, the upconverted luminescence is dominantly contributed either by energy-transfer upconversion or by excited-state absorption. The relative intensities of upconverted luminescence are discussed using Judd-Ofelt theory.

DOI: 10.1103/PhysRevB.66.035103 PACS number(s): 78.55.−m, 42.70.−a

I. INTRODUCTION

Crystals of $Y_3Al_5O_{12}$-doped triply ionized ions of erbium (Er^{3+}) are well-known laser materials that can emit in the infrared and visible ranges[1–3] and involve a large variety of upconversion processes taking place due to the rich energy level structure of Er^{3+} ions.[4,5] In contrast to chloride, bromide, and iodide compounds, such as $RbGd_2X_7$ (X=Cl, Br), K_2LaX_5 (X=Cl, Br), and $Cs_3Lu_2X_9$ (X=Cl, Br, I), which are all very sensitive to moisture and therefore need handling in dry boxes and protection during measurement and storing,[6] the compounds used in this study commonly referred to as YAG is superior in terms of mechanical hardness, thermal conductivity and optical properties.[7]

Upconversion phenomena has been extensively studied on various crystals[8–12] and optical fibers doped with the Er^{3+} ions in the last decade.[13,14] Green upconversion lasing in $YAlO_3$: Er^{3+} crystals has been reported by Richard Scheps *et al.*,[7] and 551 nm laser emission has been observed in $YLiF_4$:Er^{3+}.[15–17] Whitley *et al.*[18] demonstrated room-temperature upconversion lasing in Er^{3+}-doped fluorozirconate fibers. The character and mechanism of upconversion in Er^{3+}-doped YAG crystal have been extensively discussed, but which is mainly limited in infrared and visible region.[19–21] The purpose of this paper is to investigate luminescent properties and mechanisms of ultraviolet upconversion in Er^{3+}-doped YAG crystals. The two most common excitation processes that lead to emission from energy states higher than the terminating state of the first pump-absorption step are pump excited-state absorption (ESA) and energy-transfer upconversion (ETU).[22]

Upconversion of Er^{3+} is well known for excitation into three multiplets in the infrared: $^4I_{13/2}$ ($\approx$1.55 μs), $^4I_{11/2}$ ($\approx$980 nm), and $^4I_{9/2}$ ($\approx$800 nm).[23,24] In the visible-to-ultraviolet upconversion processes, the $^4S_{3/2}$ ($\approx$545 nm) state is of most important for serving as an intermediate excited state due to its longer lifetime than that of other states in the visible range.[11,25] In this study, we report on the generation of ultraviolet upconversion signals in Er^{3+}-doped YAG crystals upon $^4S_{3/2}$ excitation by a tunable OPO laser excitation. For the interpretation of short-wavelength luminescence, we measured the decay profile of upconverted luminescence, the dependence of intensity of upconverted luminescence on pump power, absorption and excitation spectroscopy.

The experimental apparatus is described in Sec. II and the experimental results are given in Sec. III. In Sec. IV the results of Sec. III are analyzed and discussed. Finally some conclusions are drawn in Sec. V.

II. EXPERIMENT

The YAG: Er^{3+} (8.4 mol. %) crystal grown by a conventional Czochralski technique in Changchun Institute of Applied Chemistry of China, has a size of $1.0\times1.0\times1.0$ cm^3. The YAG sample has a cubic space-group symmetry O_h^{10}, and the Er^{3+} ions substitute Y^{3+} ions on the dodecahedral sites having D_2 symmetry.[26]

The absorption spectrum of the crystal was measured by a Perkin-Elmer Lambda-9 UV–visible–near-infrared spectrophotometer with a resolution of 0.2 nm. A nanosecond laser system was employed to produce the excitation laser pulses, and this laser system consists of a Nd:YAG pump source and a tunable OPO laser. The Nd:YAG laser (Continuum Precision II 8000) is a Q switched and injection seeded at a repetition of 10 Hz and provides a frequency tripled 355 nm light beam for pumping the tunable OPO laser (Continuum Sunlite EX) with 6 ns duration. The wavelength of the laser system was calibrated by Burleigh Pulsed Wavemeter (WA-4500). To obtain the required violet and UV wavelengths in the 240–450 nm regions, frequency doubling of the OPO laser output in two BBO crystals (continuum FX-1 UV frequency extension) was used. Following pulsed excitation, the fluorescence was collected at right angles to the incident beam by a 4-cm-diameter, 10-cm-focal-length quartz lens passing an UV band-pass filter (Schott BG-24) onto the entrance slit of the calibrated monochromator. The exit slit of the monochromator was equipped with a photomultiplier tube (Hamamatsu R3896). For decay profile measurements of upconverted luminescence, the signals from photomultiplier tube were recorded by a Tektronix TDS 620B 500 MHz digital real-time oscilloscope, while for luminescence and excitation spectra measurements, a gated integrators and boxcar integrators (Stanford Research Systems SR250) was used. Both of them were triggered by a photoelectric diode.

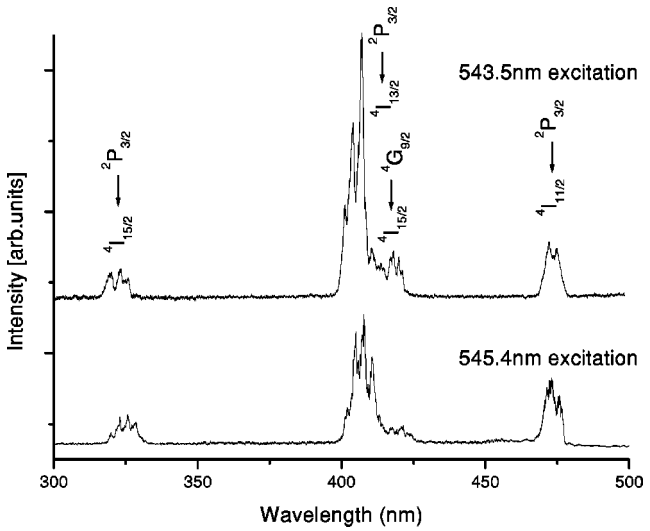

FIG. 1. Upconversion luminescence spectra of YAG: 8.4% Er^{3+} at room-temperature normalized to an equal integrated intensity of the transition under 543.5 (top) and 545.3 nm (bottom) excitation.

Through GPIB and RS232 cables the signals could be transferred to a personal computer, where the analyses of the decay curve and the spectra were performed in direct connection with the experiment. All experiments were performed at room temperature.

III. RESULTS

Figure 1 shows the upconverted luminescence spectra of the YAG: 8.4% Er^{3+} sample under two excitation wavelengths 543.5 nm (18 400 cm^{-1}) and 545.4 nm (18 335 cm^{-1}), which have been corrected by the instrumental response including the filter. For comparison, the two curves were scaled to an equal integrated intensity of the $^2P_{3/2} \rightarrow {}^4I_{15/2}$ transition. The upper spectrum was excited at 543.5 nm, and the lower at 545.4 nm. Three emission bands around 320, 410, and 470 nm in Fig. 1 were assigned to the transitions from $^2P_{3/2}$ into the ground state $^4I_{15/2}$ and the first two excited states $^4I_{13/2}$ and $^4I_{11/2}$. By fixing the detection wavelength at 321.9 and 407.8 nm and scanning the laser wavelength, we obtained the excitation spectra as shown in Fig. 2 (middle and bottom traces), in which the corresponding absorption spectra (top trace) is also included. The spectra were scaled to the same height of the peak at 545.4 nm. Several peaks of the excitation spectra coincide with the absorption spectra, but the relative intensities are different from that of absorption spectrum.

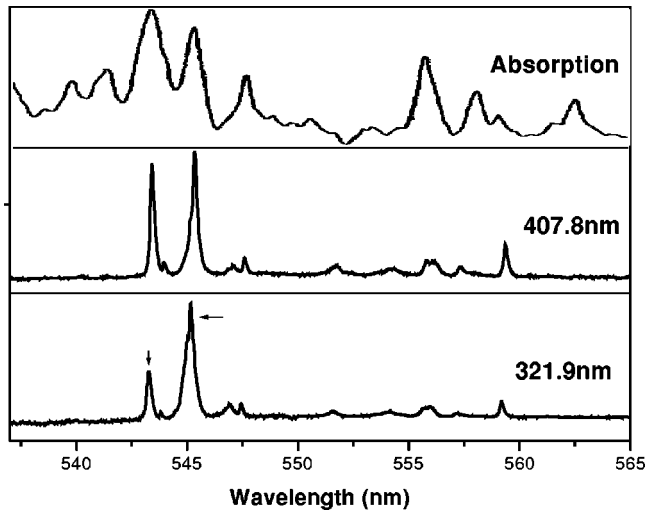

FIG. 2. Excitation spectra in the region between 537 and 565 nm for YAG: 8.4% Er^{3+}, detecting 407.8 (middle) and 321.9 nm (bottom) upconverted luminescence. The top trace shows absorption spectrum of $^4I_{15/2} \rightarrow {}^4S_{3/2}$ transition.

In order to determine the mechanism of the upconversion process, the decay profiles after pulsed excitation have been measured by monitoring luminescence at 321.9, 408.2, and 475.3 nm, as shown in Fig. 3. The insets show the same data but in a semilogarithmic representation. Two different excitation wavelengths, as indicated by the arrows in Fig. 2, were used: 543.5 nm (top) and 545.4 nm (bottom). It can be seen in Fig. 3 that the decay profiles of upconverted luminescence at 321.9, 408.2, and 475.3 nm are almost the same. The top curves exhibit a clear rise time of 2 μs, whereas the bottom curves have no rise but an almost exponential decay with the lifetime of 6.5 μs, which resembles the lifetime (5.8 μs) of

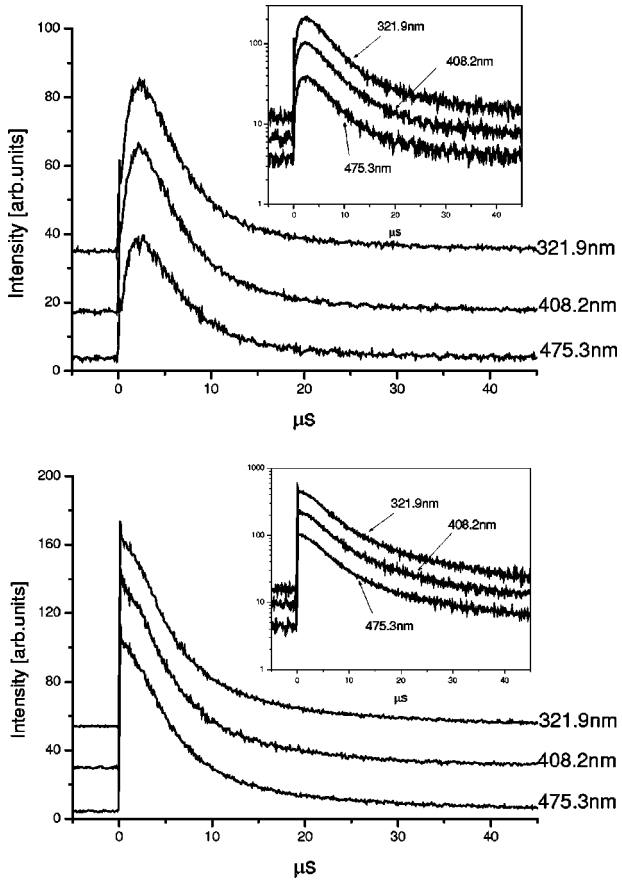

FIG. 3. Decay profiles of the upconverted luminescence at 321.9, 408.2, and 475.3 nm in YAG: 8.4% Er^{3+} after a short (6 ns) excitation. Excitation wavelengths were 543.5 (top) and 545.4 nm (bottom) as indicated by the arrows in Fig. 2. The insets show the same data but in a semilogarithmic representation.

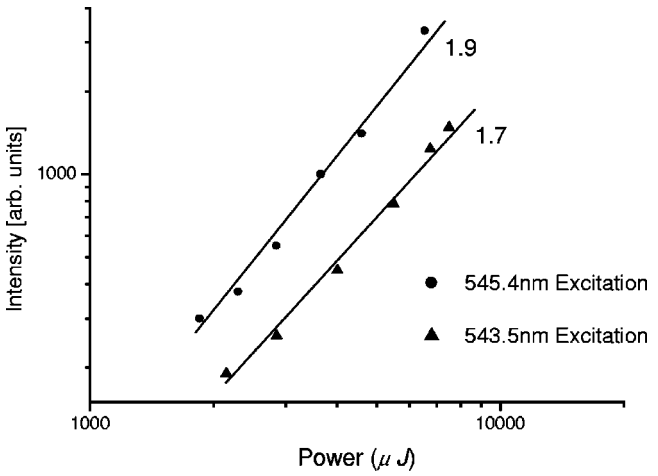

FIG. 4. Measured emission intensities from the $^2P_{3/2}$ state at 321.9 nm, in YAG: 8.4% Er^{3+} vs pump power. The numbers denote the slopes in double-logarithmic representation under 543.5 (1.7) and 545.4 nm (1.9) excitation, respectively.

the $^2P_{3/2}$ state by direct excitation measurement. The power dependence of upconverted luminescence at 321.9 nm was measured by inserting different neutral density filters in the pump beam. The results are shown in Fig. 4 in double logarithmic scale, and the slopes of plot for two excitation wavelengths (543.5 and 545.4 nm) are 1.7 and 1.9, respectively.

IV. DISCUSSION

A relevant part of schematic energy state diagram of Er^{3+} ion based on spectroscopic data reported by Gruber[27] is shown in Fig. 5. From Fig. 5 and the decay profiles shown in Fig. 3, it can be confirmed that the observed luminescence spectra come from the $^2P_{3/2}$ state. According to the power dependence (Fig. 4) with the slopes of 1.7 and 1.9, it reflects a two-step upconverted process. Therefore, to populate the $^2P_{3/2}$ state can be considered as three possible processes. One is an ESA process, which consists of two consecutive

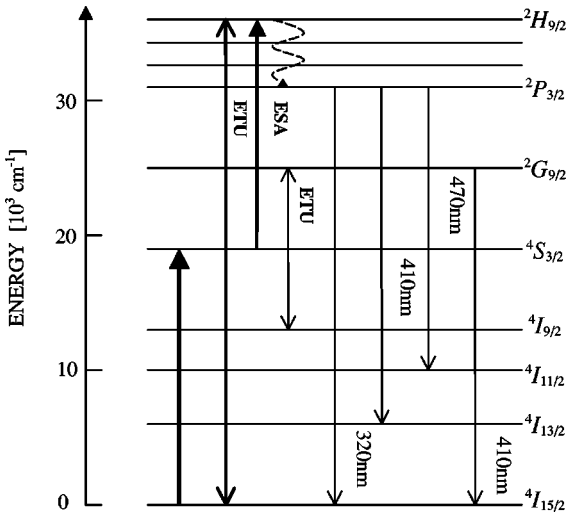

FIG. 5. Simplified energy-level diagram for Er^{3+} ion showing upconversion mechanism and emission transitions.

excitation steps on a single ion and takes place when an Er^{3+} ion in exited state $^4S_{3/2}$ absorbs another photon to populate $^2H_{9/2}$. Subsequent nonradiative relaxation from the $^2H_{9/2}$ state populates the $^2P_{3/2}$ state resulting in the upconverted luminescence. The other one is ETU process, in which two Er^{3+} ions in the $^4S_{3/2}$ state interact resulting in that the energy of an ion in the intermediate state is transferred nonradiatively onto another ion thereby exciting it into a higher excited state $^2H_{9/2}$, and following a population of $^2P_{3/2}$ state. The third process is avalanche upconversion, which can be excluded in our case because none of the typical signature for this process could be found.

Time-dependent measurements following a pulsed excitation provide the first possibility to distinguish between these two mechanisms.[6,20,21] ESA has to take place during the excitation pulse, whereas the ETU process can process after the $^4S_{3/2}$ excitation by the laser pulse. Therefore, the lifetime of upconverted luminescence upon ETU exhibits an observable rise time of 2 μs, while ESA upconversion process results in a decay profile without rise time and shows an almost exponential decay behavior similar to that by direct excitation. It can be clearly seen from Fig. 3 that excitation at 543.5 nm reveals an ETU upconversion process, whereas 545.4 nm excitation is an ESA upconversion process. However, the semilogarithmic plots of the lower trace in Fig. 3 show an impure exponential decay behavior. This reflects a small fraction of ETU upconversion also for 545.4 nm excitation. Conversely, the upper trace in Fig. 3, which is dominantly due to ETU, is slightly contaminated by an ESA process, because its rise does not start from zero intensity. The second identification to distinguish the two processes can be obtained from absorption and excitation spectra in Fig. 2. In the case of an energy-transfer upconversion, the $^4S_{3/2}$ multiplet acts as a sensitizer for both ions and therefore the excitation spectra similar to the $^4I_{15/2} \rightarrow {}^4S_{3/2}$ absorption spectra is expected. However, for an ESA process, additional resonance transitions corresponding to $^4S_{3/2} \rightarrow {}^2H_{9/2}$ should be considered. Looking at the two peaks at 545.4 and 543.5 nm in Fig. 2 and comparing with the absorption spectra (upper trace), the absorption at 543.5 nm is stronger than that at 545.4 nm, whereas in the excitation spectra the peak at 543.5 nm is smaller than that at 545.4 nm. This implies that excitation at 545.4 nm contained an ESA process, i.e., there exists a second-step resonance. This can be confirmed by comparing the energy intervals between $^4S_{3/2}$ and $^2H_{9/2}$ Stark sublevels with these two excitation wavelengths, from which we found that excited at 545.4 nm more close to the resonance wavelength. Based on experimental evidences presented in decay profiles and excitation spectra, we conclude that excitation at 543.5 nm essentially leads to an ETU process, whereas 545.4 nm excitation leads to an ESA upconversion process.

Figure 2 also appears that the individual peaks in excitation spectra are narrower than the absorption peaks, which is due to the higher resolution (0.05 nm) of monochromator used for excitation spectra measurement than that (0.2 nm) of spectrophotometer used in absorption.

To explain the intensity ratio of three upconversion luminescence (320, 410, and 470 nm), we calculated the transi-

TABLE I. Transition probabilities of the $^2P_{3/2}$ state, and Judd-Ofelt parameters of Er^{3+}, in YAG: 8.4% Er^{3+} crystal.

J	J'	$A_{JJ'}(S^{-1})$
$^2P_{3/2}$	$^4I_{15/2}$	527
$^2P_{3/2}$	$^4I_{13/2}$	1805
$^2P_{3/2}$	$^4I_{11/2}$	1144
Intensity parameters (cm^2)		
Ω_2		0.79×10^{-20}
Ω_4		1.19×10^{-20}
Ω_6		1.08×10^{-20}

tion probability from $^2P_{3/2}$ to $^4I_{15/2}$, $^4I_{13/2}$, and $^4I_{11/2}$ using the Judd-Ofelt theory. Judd-Ofelt parameters Ω_2, Ω_4, and Ω_6 of Er^{3+} in YAG were calculated by an empirical formula.[28] The reduced matrix element of the tensor operator $U^{(2)}$, $U^{(4)}$, and $U^{(6)}$ were obtained from Ref. 29. The calculated transition probabilities are listed in Table I together with the parameters Ω_t. The calculated intensity ratio of three emission bands is approximately 1:4:2.5. If all the upconversion luminescence at 320, 410, 470 nm come from the $^2P_{3/2}$ state, the experimental intensity ratios for these three bands will be the same as calculated results, regardless of ETU or ESA upconversion mechanisms. It can be obtained from Fig. 1 that the experimental luminescence intensity ratio (1:4:2.2) at 545.4 nm excitation is good agreement with the theoretical results, but at 543.5 nm excitation, the ratio is 1:6:2.1. This means that there is an additional contribution to the 410 nm band at 543.5 nm excitation wavelength. We found a possibility for this additional signal as follows. According to spectroscopic data reported by Gruber,[27] the energy differences between the multiplets $^4I_{9/2}-{}^4S_{3/2}$ and $^4S_{3/2}-{}^2G_{9/2}$ are almost equal, whereas the luminescence of $^2G_{9/2}\rightarrow{}^4I_{15/2}$ transition around 410 nm overlaps partially with that of $^2P_{3/2}\rightarrow{}^4I_{13/2}$ transition. Therefore the ETU upconversion process $(^4S_{3/2}\rightarrow{}^4I_{9/2})+(^4S_{3/2}\rightarrow{}^2G_{9/2})$ is possible to contribute the additional upconverted luminescence around 410 nm under 543.5 nm excitation. This assumption can also be supported by the excitation spectra in Fig. 2. It is seen from Fig. 2 that the excitation intensity at 543.5 nm relative to the excitation intensity at 545.4 nm is considerably smaller for 321.9 nm emission than for 407.8 nm emission. If there is not an additional contribution to the 407.8 nm at 543.5 nm excitation, the intensity ratios of the two individual peaks in two excitation spectra should be the same. This provides another identification to the $(^4S_{3/2}\rightarrow{}^4I_{9/2})+(^4S_{3/2}\rightarrow{}^2G_{9/2})$ upconversion process.

V. CONCLUSION

In this paper, we have observed the ultraviolet and violet upconversion luminescence in $Y_3Al_5O_{12}$: Er^{3+} (8.4 at.%) crystal upon $^4S_{3/2}$ excitation. In order to understand the upconversion mechanism, we measured decay profile of upconverted luminescence, power dependence, excitation, and luminescence spectra. With the arguments involved in Sec. IV, two possible upconversion processes ETU and ESA exist depending on excitation wavelength as shown in Fig. 5. At 543.5 nm excitation, Er^{3+} ions in the ground state were pumped to the $^4S_{3/2}$ state by GSA process, then through ETU process, two ions in the $^4S_{3/2}$ state to produce an ion in the $^2H_{9/2}$ state and the other into the ground state. Subsequent nonradiative relaxation from the $^2H_{9/2}$ state populates the $^2P_{3/2}$ state. An additional upconversion process $(^4S_{3/2}\rightarrow{}^4I_{9/2})+(^4S_{3/2}\rightarrow{}^2G_{9/2})$ also occurs at this excitation wavelength. At 545.4 nm excitation, Er^{3+} ions can also be excited from the ground state to the $^4S_{3/2}$ state subsequently Er^{3+} ion in the $^4S_{3/2}$ state absorbs another photon to $^2H_{9/2}$, resulting in the ESA upconversion luminescence. Because of YAG crystal is an excellent laser host material, the observation of ultraviolet and violet luminescence in YAG: Er^{3+} is benefit for the investigation of upconversion lasing in short wavelength.

ACKNOWLEDGMENTS

The authors wish to thank Professor S.Y. Zhang of Changchun Institute of Applied Chemistry, China, for providing the crystals. This work was financially supported by the National Natural Science Foundation of China (Grant No. 10074020).

[1] F. Tong, W.P. Risk, R.M. Macfarlane, and W. Lenth, Electron. Lett. **25**, 1389 (1989).
[2] T.J. Whitley, C.A. Millar, R. Wyatt, M.C. Brierley, and D. Szebesta, Electron. Lett. **27**, 1785 (1991).
[3] M. Pollnau, E. Heumann, and G. Huber, Appl. Phys. A: Solids Surf. **54**, 404 (1992).
[4] C.L. Pope, R.B. Reddy, and S.K. Nash-Stevenson, Opt. Lett. **22**, 295 (1997).
[5] J. Breguet, A.F. Umyskow, S.G. Semenkov, W. Lüthy, H.P. Weber, and I.A. Shcherbakov, IEEE J. Quantum Electron. **28**, 2563 (1992).
[6] T. Riedener, P. Egger, J. Hulliger, and H.U. Güdel, Phys. Rev. B **56**, 1800 (1997).
[7] R. Scheps, IEEE J. Quantum Electron. **30**, 2914 (1994).
[8] W.Q. Shi, M. Bass, and M. Birnbaum, J. Opt. Soc. Am. B **6**, 23 (1989).
[9] A. Lupei, V. Lupei, S. Georgescu, I. Ursu, V.I. Zhekov, T.M. Murina, and A.M. Prokhorov, Phys. Rev. B **41**, 10 923 (1990).
[10] S. Georgescu, V. Lupei, A. Lupei, V.I. Zhekov, T.M. Murina, and M.I. Studenkin, Opt. Commun. **81**, 186 (1991).
[11] D.N. Patel, R.B. Reddy, and S.K. Nash-Stevenson, Appl. Opt. **37**, 7805 (1998).
[12] S.R. Lüthi, M. Pollnau, H.U. Güdel, and M.P. Hehlen, Phys. Rev. B **60**, 162 (1999).
[13] M. Takahashi, M. Shojiya, R. Kanno, Y. Kawamoto, K. Kadono, T. Ohtsuki, and Peyghambarian, J. Appl. Phys. **81**, 2940 (1997).
[14] M. Tsuda, K. Soga, H. Inoue, S. Inoue, and A. Makishima, J. Appl. Phys. **85**, 29 (1999).

[15] R.A. McFarlane, Opt. Lett. **16**, 1397 (1991).
[16] R. Brede, E. Heumann, J. Koetke, T. Danger, G. Huber, and B. Chai, Appl. Phys. Lett. **63**, 2030 (1993).
[17] F. Heine, E. Heumann, T. Danger, T. Schweizer, G. Huber, and B. Chai, Appl. Phys. Lett. **65**, 383 (1994).
[18] T.J. Whitley, C.A. Millar, R. Wyatt, M.C. Brierley, and D. Szebesta, Electron. Lett. **27**, 1785 (1991).
[19] X. Zou and T. Izumitani, J. Non-Cryst. Solids **162**, 68 (1993).
[20] M. Malinowski, M.F. Joubert, and B. Jacquier, Phys. Rev. B **50**, 12 367 (1994).
[21] M.P. Hehlen, G. Frei, and H.U. Güdel, Phys. Rev. B **50**, 16 246 (1994).
[22] M. Pollnau, D.R. Gamelin, S.R. Lüthi, H.U. Güdel, and M.P. Hehlen, Phys. Rev. B **61**, 3337 (2000).
[23] A. Lupei, V. Lupei, S. Georgescu, I. Ursu, V.I. Zhekov, T.M. Murina, and A.M. Prokhorov, Phys. Rev. B **41**, 10 923 (1990).
[24] B. Majaron, T. Rupnik, and M. Lukac, IEEE J. Quantum Electron. **32**, 1636 (1996).
[25] H. Xu, Z. Dai, and Z. Jiang, Eur. Phys. J. D **17**, 79 (2001).
[26] J.B. Gruber, M.E. Hills, R.M. Macfarlane, C.A. Morrison, and G.A. Turner, Chem. Phys. **134**, 241 (1989).
[27] J.B. Gruber, J.R. Quagliano, M.F. Reid, F.S. Richardson, M.E. Hills, M.D. Selzer, S.B. Stevens, C.A. Morrison, and T.H. Allik, Phys. Rev. B **48**, 15 561 (1993).
[28] Q.Y. Wang, S.Y. Zhang, and Y.Q. Jia, J. Alloys Compd. **202**, 1 (1993).
[29] A.A. Kaminskii, V.S. Mironov, A. Kornienko, S.N. Bagaev, G. Boulon, A. Brenier, and B.D. Bartolo, Phys. Status Solidi A **151**, 231 (1995).